J. Plasma Physics (2010), *vol.* 76, *part* 5, *pp.* 709–734. © Cambridge University Press 2010
doi:10.1017/S002237781000022X

Spatio-temporal evolution of thin Alfven resonance layer

I. S. DMITRIENKO

Institute of Solar-Terrestrial Physics SB RAS, P/O Box 291, Irkutsk 664033, Russia
(dmitrien@iszf.irk.ru)

(Received 28 May 2009, revised 19 March 2010 and accepted 7 April 2010,
first published online 7 May 2010)

Abstract. We describe the spatio-temporal evolution of one-dimensional Alfven resonance disturbance in the presence of various factors of resonance detuning: dispersion and absorption of Alfven disturbance, nonstationarity of large-scale wave generating resonant disturbance. Using analytical solutions to the resonance equation, we determine conditions for forming qualitatively different spatial and temporal structures of resonant Alfven disturbances. We also present analytical descriptions of quasi-stationary and non-stationary spatial structures formed in the resonant layer, and their evolution over time for cases of drivers of different types corresponding to large-scale waves localized in the direction of inhomogeneity and to nonlocalized large-scale waves.

1. Introduction

Resonance Alfven oscillations have long been the subject of detailed study due to a variety of their related phenomena in different plasma environments, both in fusion plasma physics and space plasma physics where they are considered to be responsible for different phenomena accompanied by plasma heating and formation of fluxes of accelerated particles (Stefan 1970; Southwood 1974; Ionson 1978; Stasiewicz et al. 2000). Idea of spatio-temporal structure of disturbances in the resonance layer are valuable for diagnosing plasma processes and parameters.

This paper aims to reveal conditions for forming qualitatively different spatio-temporal structures of one-dimensional resonant Alfven disturbances and obtain their analytical descriptions in the thin Alfven resonance layer approximation. One-dimensional resonance occurs with the Alfven velocity inhomogeneity in the direction perpendicular to the undisturbed magnetic field. The thin resonance layer approximation means the use of the assumption that width of the region with the resonant Alfven disturbance (the Alfven resonance layer) is less than any spatial scale characterizing both the undisturbed environment parameters and the wave generating the Alfven resonant disturbance. In that case the wave converting into the resonant disturbance can be named as large-scale wave. The thin resonance layer occurs when energy of the wave generating the resonant disturbance is concentrated near one frequency. Consequently, we will assume that the large-scale wave is a monochromatic wave with temporal envelope. Such factors as dispersion of small-scale Alfven waves (kinetic and inertial) (Swanson 1975; Hasegawa and Boswell 1976), absorption of the Alfven disturbance (collisional or collisionless) (Chen and Hasegawa 1974), and non-stationarity of the large-scale waves are factors

https://doi.org/10.1017/S002237781000022X Published online by Cambridge University Press

of resonance detuning. They determine non-zero width of the resonance region and finite amplitude of the resonant disturbance at the resonant surface. The resonance equation in this paper, when giving a specific meaning to coefficients of this equation, describes the dispersion resonance either with model collisionless absorption or with collisional isotropic absorption. A wave propagating or localized in the direction of inhomogeneity (*e.g.* waveguide FMS waves or the Alfven surface mode) may generate the resonant disturbance.

Analytical solution to the resonance equation with arbitrary dependence of the large-scale mode amplitude on time is used for the matching of the large-scale mode through the resonance layer. We verify that matching formulae, which are obtained through the bypass of the singular point in the simplest case of a large-scale monochromatic wave described in the ideal MHD, keep their form under certain conditions. Such a matching means that the energy density flux of the large-scale wave to the resonance layer is determined only by properties of the large-scale wave and environment parameters. Resonant mode conversion of this type can be called quasi-stationary. If the large-scale mode has non-zero amplitude at the initial instance of time, solution for the resonance layer can be matched with the large-scale solution (corresponding to the quasi-stationary conversion regime) beyond the resonance layer only after a period of establishment of this regime. Time of establishment is supposed to be much shorter than any time occurring in the resonant disturbance as a result of resonance detuning factors. Thus, we may neglect its effect on evolution of the resonant disturbance. In that case, if large-scale wave is not localized in the transverse coordinate, then time behavior of its amplitude in the resonance layer is determined by time behavior of the amplitude of the wave propagating toward the resonant surface. If the large-scale mode is localized in the transverse coordinate, then its amplitude in the resonance layer may be specified as a time function decreasing exponentially from the initial instant. This function has two parameters: the initial amplitude and the decrement. These parameters may be considered arbitrary for resonant disturbance.

Analytical solutions to the resonance equation with such drivers are used to find parameters determining the character of the resonant disturbance evolution, and to describe analytically quasi-stationary and non-stationary spatial structures formed in the resonance layer and their evolution over time.

2. Alfven resonance layer equations

We will study spatio-temporal resonance structures in one-dimensional inhomogeneous plasma. The undisturbed magnetic field B_0, density ρ_0 and pressure P_0 depend only on the coordinate x. The magnetic field B_0 is unidirectional, z-axis is chosen along B_0. Disturbance is presented as a monochromatic wave with temporal envelope, *e.g.* disturbance of the magnetic field:

$$\mathbf{B} = \mathbf{b}(x, T)\exp(i\theta) + c.c., \quad \theta = -\omega t + k_z z + k_y y, \tag{2.1}$$

where *c.c.* is the complex-conjugate value, $\partial_T \ll \omega$. The Alfven resonant disturbance is formed near the surface $x = x_0$, on which condition $\omega^2 = k_z^2 V_a^2(x_0)$ is satisfied, where $V_a = \frac{B_0}{(4\pi\rho_0)^{1/2}}$ is the Alfven velocity (Chen and Hasegawa 1974; Southwood 1974).

https://doi.org/10.1017/S002237781000022X Published online by Cambridge University Press

Assuming

$$\partial_x \sim \Delta^{-1}, \quad \partial_T \sim \Delta, \tag{2.2}$$

$$\partial_z \sim \partial_y \sim \partial_t \sim \Delta^0, \tag{2.3}$$

where Δ is a small parameter ($\Delta \ll 1$) characterizing the resonance layer width (*i.e.* the region where the resonant disturbance is localized), the following equations may be written for disturbance of the form (2.1) in the resonance layer (Appendices A, B and C):

$$\partial_x P_t^{(0)} = 0, \tag{2.4}$$

$$\partial_x B_x^{(0)} = -\partial_y B_y^{(-1)}, \tag{2.5}$$

$$\begin{aligned}[-k_z^2 \left(\left(\partial_x V_a^2\right)(x_0)\right)(x - x_0) + 2\omega\partial_T\partial_\theta - dV_a^2(x_0)\,\partial_{xx}^2 \\ - aV_a^2(x_0)\,\partial_{xx}^2\partial_\theta]B_y^{(-1)}/B_0(x_0) = -V_a^2(x_0)\,k_z k_y \left(4\pi P_t^{(0)}/B_0^2(x_0)\right).\end{aligned} \tag{2.6}$$

All terms in the square bracket on the left-hand side are assumed to be small of the order of Δ. All coefficients on the left-hand side of equations do not depend on x; their values are determined by the values of undisturbed parameters on the resonant surface. The dispersion coefficient d may be positive or negative, the absorption coefficient a takes positive values only. Equation (2.6), when giving a corresponding meaning to the absorption coefficient, describes the dispersion resonance either with model collisionless absorption or with collisional isotropic absorption. Superscripts indicate order of magnitude as a degree of Δ. The disturbance in (2.4)–(2.6) is considered to be of small scale (*i.e.* changing with a scale being less or of the order of Δ). Therefore (2.4) means that the disturbance $P_t^{(0)}$ has no small-scale change; it is a large-scale wave generating the resonant disturbance. The right-hand side of (2.6) accounts for this fact. Equations (2.4) and (2.5), or their equivalent equations in another form as well as in particular cases of (2.6) used to be repeatedly obtained for the resonance layer. In this paper, the resonance equation is written with consideration for such resonance detuning factors as the Alfven wave dispersion caused by non-ideal effects, Alfven disturbance absorption and driver non-stationarity.

Let us introduce dimensionless variables

$$\omega T = \tau, \quad k_z(x - x_0) = \chi, \quad V_a/V_a(x_0) = U_a,$$

$$\mathbf{B}/B_0(x_0) = \mathbf{H}, \quad \left[4\pi P_t/B_0^2(x_0)\right] = \Psi. \tag{2.7}$$

We have $\mathbf{H}(\chi, \tau, \theta) = \mathbf{h}(\chi, \tau)\exp(i\theta) + c.c.$, $\Psi(\chi, \tau, \theta) = \psi(\chi, \tau)\exp(i\theta) + c.c.$ The x-axis direction is assumed to be chosen so that $(\partial_x U_a^2)(x_0) = -|(\partial_x U_a^2)(x_0)|$. Then (2.6) takes the following form:

$$\left[-2\partial_\tau\partial_\theta + d\partial_{\chi\chi}^2 + a\partial_{\chi\chi}^2\partial_\theta - \left(\left|\left(\partial_\chi U_a^2\right)(x_0)\right|\right)\chi\right] H_y^{(-1)} = (k_y/k_z)\Psi^{(0)}, \tag{2.8}$$

where $|\partial\chi U_a^2| = k_z^{-1}|\partial_x U_a^2|$, and, instead of (2.5), we have

$$\partial_\chi H_x^{(0)} = -(k_y/k_z)\partial_\theta H_y^{(-1)}. \tag{2.9}$$

https://doi.org/10.1017/S002237781000022X Published online by Cambridge University Press

Equation (2.8) with (2.9) considered yields of the energy balance equation in the following form:

$$\partial_\tau \int_{-\infty}^{\infty} e_R + \int_{-\infty}^{\infty} l_R = -\left[Q_L(\tau) + Q_S(\tau)\right],$$

where $e_R = \overline{(H_y^{(-1)})^2}/4\pi$ is the dimensionless energy density of the resonant disturbance (kinetic and magnetic), $l_R = -a\overline{H_y^{(-1)*}\partial_\chi\partial_\chi H_y^{(-1)}}/4\pi$ is the rate of the energy density loss caused by absorption, and $Q_L(\tau)$ and $Q_S(\tau)$ are dimensionless energy density fluxes of the large-scale wave to the resonance layer and of the small-scale Alfven wave from the resonant surface respectively:

$$Q_L(\tau) = q_L(\infty,\tau) - q_L(-\infty,\tau), \quad q_L = -\overline{\Psi^{(0)}H_x^{(0)}}/4\pi = \left(-\psi^{(0)}h_x^{(0)*} + c.c.\right)/4\pi, \tag{2.10}$$

$$Q_S(\tau) = q_S(\infty,\tau) - q_S(-\infty,\tau), \quad q_S = d\overline{H_y^{(-1)}\partial_\chi\partial_\theta H_y^{(-1)}}/4\pi$$
$$= \left(idh_y^{(-1)*}\partial_\chi h_y^{(-1)} + c.c\right)/4\pi. \tag{2.11}$$

Physical meaning of e_R, q_L, and q_S is identified with consideration for (A 4); the bar accent means the period-averaged value.

Let $\psi^{(0)} = F_0 f(\tau)$ and introduce new variables

$$2h_y^{(-1)}(\chi,\tau)k_z/\left(k_y F_0\right) = G(X,\tau), \quad \chi\left|\left(\partial\chi U_a^2\right)(x_0)\right|/2 = X$$

$$\left(\left|\left(\partial\chi U_a^2\right)(x_0)\right|/2\right)^2 d/2 = D \quad \left(\left|\left(\partial\chi U_a^2\right)(x_0)\right|/2\right)^2 a/2 = A; \tag{2.12}$$

$$D + iA = \widetilde{D}. \tag{2.13}$$

The new dispersion coefficient D as well as d may be positive or negative. The new absorption coefficient A as well as a takes only positive values.

In the notation of (2.12) and (2.13), (2.8) takes the form

$$\left[-i\partial_\tau + \widetilde{D}\partial_{XX}^2 - X\right]G = f. \tag{2.14}$$

3. Solution to the resonance equation with arbitrary driver

As the basis for solving (2.14), we will use its solution at $A = 0$, $f = const = 1, \partial_\tau = 0$. In this case we have the equation

$$\left[sign(D)\,|D|\,\partial_{XX}^2 - X\right]G = 1. \tag{3.1}$$

Function $G(X,D)$ is a dispersive stationary solution to (2.14).

Let us write $G(X,D)$ in the form $G(X,D) = -\pi(signD)|D|^{-1/3}W(\xi)$, where $\xi = (signD)X/|D|^{1/3}$ and W is a solution to the equation

$$\left[\partial_{\xi\xi}^2 - \xi\right]W = -\pi^{-1}. \tag{3.2}$$

Let us write W in the form $W = W_1 + W_0$, where W_1 is the solution to the inhomogeneous (3.2), and W_0 is the solution to the homogeneous (3.2). It is easily seen that we have $W_1 = \pi^{-1}/\xi$ as $|\xi| \to \infty$. The WKB method yields $W_0 \sim C\frac{1}{|\xi|^{1/4}}\exp[\pm i\frac{2}{3}|\xi|^{3/2}]$ as $\xi \to -\infty$ (C is a factor independent of ξ). Thus, given

https://doi.org/10.1017/S002237781000022X Published online by Cambridge University Press

$\xi \to -\infty$ (*i.e.* given $sign(D)X \to -\infty$), we have

$$G \sim C \frac{1}{|\xi|^{1/4}} \exp\left[\pm i \frac{2}{3} |\xi|^{3/2}\right]. \tag{3.3}$$

Solution (3.3) describes waves propagating along the x-axis in the direction toward or away from the resonant surface, depending on sign in the exponential function. The sign in (3.3) should be chosen in such a way that the wave could carry energy away from the resonant surface (*i.e.* projection of q_S to the axis ξ is to be negative). The energy density flux q_S carried by the wave (3.3) is determined by (2.11): $q_S = \pm |C|^2 \frac{d}{4\pi} (|(\partial \chi U_a^2)(x_0)|)(signD)/|D|^{1/3}$.

The energy density flux q_S, carried by the wave in the form of (3.3) with different signs of $D/|D|$, is directed away from the resonant surface, if the negative and positive signs in (3.3) are chosen at $D > 0$ and $D < 0$, respectively. Hence, the asymptotics $G \sim C \frac{1}{|\xi|^{1/4}} \exp[-i(signD)\frac{2}{3}|\xi|^{3/2}]$ should be chosen for G when $\xi \to -\infty$. Solution to the inhomogeneous (3.2), which provides these asymptotics of G as $\xi \to -\infty$ (*i.e.* $(signD)X \to -\infty$) and is bounded as $\xi \to \infty$ (*i.e.* $(signD)X \to \infty$), can be composed of special functions: $W(\xi) = Gi(\xi) - i(signD)Ai(\xi)$, where $Gi(\xi)$ is the Scorer's function and $Ai(\xi)$ is the Airy function. Such a solution for the dispersion of Alfven resonance equation was given in (Hasegawa and Chen 1976). When $\xi \to \infty$, we have $W(\xi) \sim Gi(\xi) \sim \pi^{-1}\xi^{-1}$ (Abramovitz 1970). Thus, the solution to (3.1) has the form

$$G(X, D) = -\pi (signD) |D|^{-1/3} [Gi(\xi) - i(signD) Ai(\xi)].$$

Using integral representations for Gi and Ai, we get integral representation for G:

$$G = i \int_0^\infty \exp\left[i\left(\frac{1}{3} D u^3 + Xu\right)\right] du.$$

The well-known asymptotic formulae for Gi and Ai (Abramovitz 1970) give asymptotics of G as $(signD)X \to -\infty$ in the following form:

$$G \sim i\pi^{1/2} |D|^{-1/3} \left|X/|D|^{1/3}\right|^{-1/4} \times \exp\left[isign(D)\left(-\frac{2}{3}\left|X/|D|^{1/3}\right|^{3/2} + \frac{\pi}{4}\right)\right]. \tag{3.4}$$

They are small-scale Alfven waves with the scale defined by $|D|^{1/3}$. When $D > 0$ and $D < 0$ (3.4) describes respectively inertial and kinetic Alfven waves.

If $f(\tau) = 1$, $\partial_\tau = 0, A \neq 0$, then (2.14) yields the equation

$$[\widetilde{D}\partial_{XX}^2 - X]G = 1. \tag{3.5}$$

It is obvious that the extension of $G(X, D)$ as a function of D into the region of complex D values with $\mathrm{Re}D > 0$ according to the formula

$$G = i \int_0^\infty \exp\left[i\left(\frac{1}{3} \widetilde{D} u^3 + Xu\right)\right] du \tag{3.6}$$

is possible; by substituting (3.6) in (3.5), we can easily verify that (3.6) is the solution to (3.5). When $D = 0$, (3.6) is the solution to (3.5) for the case when the only

https://doi.org/10.1017/S002237781000022X Published online by Cambridge University Press

non-ideal effect is absorption (collisionless or collisional), and dispersion may be ignored.

If $A \neq 0$, integration by parts suffices to obtain asymptotics G as $|X| \to \infty$. We obtain

$$G = -X^{-1}. \tag{3.7}$$

For further analysis, note that the integrand in (3.6) has complex saddle points u_p, where equation $p'(u) = 0$ is satisfied for function $p(u) = i(\frac{1}{3}\widetilde{D}u^3 + Xu)$. Their position is defined by equation $u_p^2 = -X/\widetilde{D}$. The most general approach for examining the integral with integrand of the form (3.6) is the steepest descent method enabling us to obtain approximate values of the integral in the presence of a large parameter, summarizing integrals near ends of the integration interval and those near saddle points (Olver 1974). In the dispersion case ($|D|/A \gg 1$), we reduce it to studying the effect of the phase critical point so that in this case the analysis will rely on a particular case of the steepest descent method—the stationary phase method. In the stationary phase method, approximate integral values are obtained as sums of integrals near end points of integration interval and critical points.

Let us single out phase $\phi = \frac{1}{3}Du^3 + Xu$ in p. If X is from the wave propagation region, then the phase ϕ has a positive critical point $u_c : u_c = (-X/D)^{1/2}$, $u_c > 0$. The saddle point u_{p+} with a positive real part (there is such a point at $-X/D > 0$) becomes the critical point u_c as $A \to 0$. The integral asymptotics at $A = 0$ (3.4) is determined by the integral near this point. If A is small and $|X|$ is not too large, u_{p+} is near the positive part of the real axis and influences significantly the integrand behavior in the interval of integration near the stationary phase point. The influence of saddle point u_{p+} may be taken into account using an approximate expression for the phase near $u_c = (-X/D)^{1/2}$.

By introducing variable $s = u/u_c - 1$, we rewrite p in the form

$$p = i\frac{2}{3}Xu_c + iDu_c^3\left(s^2 + \frac{1}{3}s^3\right) - \frac{1}{3}Au^3.$$

We have

$$p = i\left(\frac{2}{3}Xu_c + Du_c^3\ s^2\right) - u_c^3 A\left(\frac{1}{3} + s\right)$$

near the critical point. Scales of change in the phase and absorption part of the exponent as functions of s are $L_\phi = (|D|u_c^3)^{-1/2} = |X/|D|^{1/3}|^{-3/4}$ and $L_A = (u_c^3 A)^{-1} = (|D|/A)|X/|D|^{1/3}|^{-3/2}$, respectively. When $L_\phi \ll L_A$, *i.e.*

$$\left|X/|D|^{1/3}\right| \ll \left(|D|/A\right)^{4/3}, \tag{3.8}$$

change in the absorption part of the exponent near the critical point may be neglected; *i.e.* put $p = i\frac{2}{3}Xu_c + iDu_c^3\ s^2 - \frac{1}{3}Au_c^3$. Integral is accumulated near the critical point (at $|s| \ll 1$), if the condition

$$\left|X/|D|^{1/3}\right| \gg 1 \tag{3.9}$$

is met. When conditions (3.8) and (3.9) are fulfilled ((3.8) and (3.9) may be jointly valid when $|D|/A \gg 1$), we get that the integral in the vicinity of u_c contributes to G

https://doi.org/10.1017/S002237781000022X Published online by Cambridge University Press

in the form of a small-scale absorbed wave G_S:

$$G_S = |D|^{-1/3}\ \ i\pi^{1/2}\left|X/|D|^{1/3}\right|^{-1/4}\exp\left[-\frac{1}{3}\frac{A}{D}\left|X/|D|^{1/3}\right|^{3/2}\right]$$

$$\times\exp\left[isign(D)\left(-\frac{2}{3}\left|X/|D|^{1/3}\right|^{3/2}+\frac{\pi}{4}\right)\right]. \tag{3.10}$$

It is easy to see that the integral near the integration end point $u = 0$ yields (3.7). By adding (3.10) to the right-hand side of (3.7), we get $G = -X^{-1} + G_S$. As is seen, $G = G_S$ when $A \neq 0$ at not too large $|X|$ from the wave propagation region $(-X/D > 0)$. The condition opposite to (3.8) is met when $A \neq 0$, $-X/D > 0$, and $|X|$ values are quite large. In this case, the change of p in the vicinity of the critical point is determined by the absorption part of p; thus, effect of the critical point is insignificant, and we get (3.7).

The solution (3.6) allows (2.14) to be easily solved by means of Fourier transform with respect to time. Let us denote

$$w(X,v) = \int_{-\infty}^{\infty} G(X,\tau)\,e^{-iv\tau}d\tau,\ \ F(v) = \int_{-\infty}^{\infty} f(\tau)\,e^{-iv\tau}d\tau.$$

Then

$$G(X,\tau) = \frac{1}{2\pi}\int_{-\infty}^{\infty} e^{iv\tau}w(X,v)\,dv,\quad f(\tau) = \frac{1}{2\pi}\int_{-\infty}^{\infty} e^{iv\tau}F(v)\,dv.$$

As both G and f can be considered as ordinary or generalized functions. Applying the Fourier transform to (2.14) we obtain

$$[v - X + \widetilde{D}\partial_X\partial_X]w = F.$$

The solution to this equation that satisfies the condition of carrying energy by the wave away from the resonant surface is

$$w = iF\int_{-\infty}^{\infty}\exp\left[i\left(\frac{1}{3}\widetilde{D}u^3 + (X-v)\,u\right)\right]du.$$

The inverse Fourier transform due to the convolution theorem yields the solution to (2.14) in the following form:

$$G(X,\tau) = i\int_0^{\tau} f(\tau-u)\exp\left[i\left(\frac{1}{3}\widetilde{D}u^3 + Xu\right)\right]du. \tag{3.11}$$

It should be noted that the solution of the form (3.11) for a dissipative case $(A \neq 0, D = 0)$ of the (2.14) was obtained in Ruderman et al. (1995). The method of obtaining the time-dependent solution in Ruderman et al. (1995) (as well as the stationary solutions in Tirry and Goossens (1996) is based on the Fourier transform with respect to χ. Because terms of the (2.14), (3.1) insufficiently rapid decrease as $|X| \to \infty$ for the ordinary Fourier transform, the Fourier transform in the sense of generalized functions can only be used. Choice of unique solution in Ruderman et al. (1995) based on elimination of the part of the solution, that have indefiniteness, and physical meaningless of which is evident when $A \neq 0$. Method of Fourier transform with respect to χ is also applicable for the case $D \neq 0$ and lets to obtain in this case, if $A \neq 0$, both the solution (3.6) and (3.11) the same way as in Ruderman et al. (1995). When $A = 0$, uniqueness of the solutions of the (2.14), (3.1) is defined

https://doi.org/10.1017/S002237781000022X Published online by Cambridge University Press

by the condition, that the energy density flux q_s is directed away from the resonant surface, the use of which requires involvement of the wave asymptotics. This can be avoided by considering the solution at $A = 0$ as the limit of solution with $A \neq 0$ when $A \to 0$. In such approach, the method of Ruderman et al. (1995) gives the shortest way to the solution of (2.14) for any A and D. We obtain the solution (3.11) for any A, which, as follows from the above, coincides with the solution obtained for the case $D \neq 0$ from the condition of carrying energy away by the small-scale wave. Using Fourier transform with respect to time supplements this solution with the evidence that in the case $A = 0$ (as well as in the $A \neq 0$) it gives the right direction of the energy density flux.

We will further consider the case when $f(\tau) = 0$ when $\tau < 0$. Then we have

$$G = i \int_0^{\tau} f(\tau - u) \exp\left[i\left(\frac{1}{3}\widetilde{D}u^3 + Xu\right)\right] du. \tag{3.12}$$

Let us denote times and lengths, providing by integrand in (3.12). We will use τ_D and τ_A for dispersion and absorption times: $\tau_D = |D|^{-1/3}$ and $\tau_A = A^{-1/3}$. Besides, driver can provide its time; let us denote it by τ_f. The length $\Delta_\alpha : \Delta_\alpha = \tau_\alpha^{-1}$ corresponds to each time τ_α.

Now we can verify applicability of matching formulae obtained for a large-scale monochromatic wave with the bypass rule of the singularity for the case of evolving resonant disturbance (3.12). When the coefficients characterizing large-scale disturbances are functions of τ, such formulae ((D 5), (D 6)) can be written in the form (D 8) and (D 9). Equation (2.4) obviously gives condition of the total pressure invariability through the resonance layer (D 8). Formula giving the jump h_x in the resonance layer is consequence of (2.5). Integrating (2.9) on X with account for the change of variables (2.12) and for the expression (3.12) yields

$$h_x(X_0, \tau) - h_x(-X_0, \tau) = 2\, F_0 \frac{k_y^2}{k_z^2} \left|\left(\partial\chi U_a^2\right)(x_0)\right|^{-1} \int_0^{\tau X_0} \frac{1}{r} f\left(\tau - \frac{r}{X_0}\right) \exp\left[i\left(\frac{1}{3}\left(\widetilde{D}/X_0^3\right) r^3\right)\right] \sin(r)\, dr,$$

where $r = X_0 u$, $X_0 > 0$. We will assume that $f(\tau)$ is a continuous function. In that case

$$\lim_{X_0 \to \infty} 2 \int_0^{\tau X_0} \frac{1}{r} f\left(\tau - \frac{r}{X_0}\right) \exp\left[i\left(\frac{1}{3}\left(\widetilde{D}/X_0^3\right) r^3\right)\right] \sin(r)\, dr = 2f(\tau) \int_0^{\infty} \frac{\sin r}{r} dr = f(\tau)\pi,$$

then

$$\Delta h_x(\tau) = \lim_{X_0 \to \infty} \left(h_x(X_0) - h_x(-X_0)\right) = -\pi F_0 \frac{k_y^2}{k_z^2} \left[\partial_x U_a^2(x_0)\right]^{-1} f(\tau) \tag{3.13}$$

at $\tau \neq 0$. According to (D 10), matching formula obtained with the bypass rule (D 9) as well as formula for the energy density flux of the large-scale mode to the resonance layer (D 11) correspond to the jump of h_x (3.13). This resonance absorption regime may be classified as quasi-stationary or quasi-monochromatic. Matching formulae for the visco-resistive resonance case were given for the stationary case in Einaudy

https://doi.org/10.1017/S002237781000022X Published online by Cambridge University Press

and Mok (1985), decaying mode in Goossens et al. (1995) and Ruderman et al.(1995), and non-stationary resonance in Dmitrienko (1999).

Of special interest is the case when the resonant disturbance is generated by the large-scale mode localized on the transverse coordinate. Let us show that evolution of the resonant disturbance generated by the localized mode, converting into the resonant disturbance, can be described by (3.12) with a certain driver $f(\tau)$. As the property of the localized mode is that it obtains non-zero amplitude under action of initial disturbance (Appendix E), let us consider the jump of h_x, supposing $f(0) \neq 0$. We have

$$h_x(X_0) - h_x(-X_0) = 2f(0) F_0 \frac{k_y^2}{k_z^2} \left|\left(\partial\chi U_a^2\right)(x_0)\right|^{-1} \int_0^{X_0\tau} \frac{1}{r} \sin r dr$$

as $\tau \to 0$.

The right-hand side takes values close to $\Delta h_x(\tau)$ (3.13) when integral oscillations are small (*i.e.* when $X_0\tau \gg 1$). This condition can be specified using tabular values of Sine Integral $\mathtt{Si}(X_0\tau)$: we obtain $|\mathtt{Si}(X_0\tau) - \frac{\pi}{2}| \lessapprox 10\%$ when $X_0\tau \geqslant 2$. Influence of the resonant disturbance on the transversely localized large-scale mode results in the jump of h_x (3.13), when the integral is accumulated in the domain of applicability of (2.4)–(2.6) (then $X_0 \to \infty$ has meaning). Let us write this condition in the form $X_0 \ll L$, where only facts, that L is independent of parameters determining the resonance layer width and that $L \gg \Delta$, are important for the problem of description of the resonant disturbance evolution. Let us denote the time of establishment of conversion regime, which corresponds to the jump (3.13), by τ_e. Formula (3.13) can be used when $\tau \gtrapprox \tau_e$. We have $\tau_e = 2\alpha L^{-1}$ and $\alpha \gg 1$. For instance, if the only condition of applicability of (2.4)–(2.6) is localization of the resonant disturbance in the scale which is less then the scale of large-scale wave, then $L = \frac{2k_z}{k_y}(\partial\chi U_a^2)(x_0)$ and $\tau_e = \alpha\frac{k_y}{k_z}|(\partial\chi U_a^2)(x_0)|^{-1}$. In what follows we will assume $\tau_e \ll \min\{\tau_D, \tau_A, \tau_f\}$.

Time behavior of the amplitude of the localized large-scale mode, corresponding with the jump (3.13), is of the form : $f(\tau) \propto \exp[-\gamma\tau]$ (Appendix E). On the one hand, if resonant absorption is sufficiently small, then we can set $f(\tau) \approx f(0)$ at the establishment stage of quasi-stationary resonant absorption (Appendix E); on the other hand, if $\tau_e\gamma \ll 1$, then we have $\exp[-\gamma\tau] \approx 1$ at $\tau \lesssim \tau_e$. Therefore we may consider $\exp[-\gamma\tau]$ as an applicable model function when $\tau < \tau_e$ and to set

$$f(\tau) = \exp[-\gamma\tau], \quad \tau \geqslant 0, \quad f(\tau) = 0, \ \tau < 0. \tag{3.14}$$

Thus, we have in the case of the localized large-scale mode

$$G = i\exp[-\gamma\tau] \int_0^\tau \exp\left[\left(i\frac{1}{3}\widetilde{D}u^3 + iXu + \gamma u\right)\right] du. \tag{3.15}$$

In the case of the non-localized mode with quite small resonance absorption, we can neglect its effects on the large-scale wave amplitude in the resonance layer and set $f(\tau) = c_0 C_I(\tau)$, where $C_I(\tau)$ is the amplitude of the wave propagating toward the resonant surface and c_0 is a constant factor. This factor is determined by the parameters characterizing the large-scale wave and environment. In this case, the driver may be specified as an arbitrary time function. We will assume that the driver has finite duration and set $f(\tau) = f_1(\tau)$, $f_1(\tau) = 0$ when $\tau > \tau_1$. Then we have

https://doi.org/10.1017/S002237781000022X Published online by Cambridge University Press

(3.12) with f_1 instead of $f(\tau)$ when $\tau \leqslant \tau_1$ and

$$G = i \int_{\tau-\tau_1}^{\tau} f_1(\tau - u) \exp\left[i \left(\frac{1}{3} \widetilde{D} u^3 + Xu \right) \right] du, \tag{3.16}$$

when $\tau > \tau_1$.

4. Spatio-temporal structures of Alfven resonant disturbances at various relations of resonance detuning parameters

As is seen from (3.12), we have $G = i\tau$, if τ is smaller than any time τ_α and $\tau \ll |X|^{-1}$. If $|\widetilde{D}|^{1/3}\tau \ll 1, \tau \ll \tau_f$, and $|\widetilde{D}|\tau^2 \ll |X|$, we can neglect non-ideal effects in (3.12) and set $f(\tau) = f(0)$. Then we get a non-stationary solution of the form $G = -\frac{1}{X} f(0) + \frac{1}{X} f(0) \exp(iX\tau)$ for the initial evolution stage. It is easily seen that if $A = 0$, the non-stationary disturbance persists quite far from the resonant surface at any τ. Asymptotics G as $|X| \to \infty$ at any τ can be determined using integration by parts, if $f(\tau)$ is a bounded function and minimal scale of its change is non-zero. We obtain

$$G = G_I + G_E, \tag{4.1}$$

$$G_I = -\frac{1}{X} f(\tau), \quad G_E = \frac{1}{X} f(0) \exp\left(i \frac{1}{3} D\tau^3 - \frac{1}{3} A\tau^3 + iX\tau \right).$$

Obviously, G_I describes amplitude of induced oscillations. Function $G_0 = \exp\left[i \left(\frac{1}{3} D\tau^3 - \frac{1}{3} A\tau^3 + X\tau \right) \right]$ is the non-stationary solution to the homogenous equation (2.14); hence G_E describes eigen oscillations with the spatial envelope. Eigen oscillations have time-dependent dispersion frequency shift $\Delta\Omega_D(\tau) : \Delta\Omega_D(\tau) = -D\tau^2$. It provides frequency increase and decrease with time at $D < 0$ and $D > 0$, respectively. Absorption causes the disturbance decay; absorption decrement $\Gamma_A(\tau)$ appears: $\Gamma_A(\tau) = A\tau^2$. Thus, G retains its non-stationary character far from the resonant surface until eigen oscillations decay due to absorption.

Let us note that (3.12) is the superposition of eigen oscillations generated by the driver at various instants of time. The integral near the lower limit of integration represents induced oscillations, while the integral near the upper limit represents eigen oscillations generated by the driver at the initial instant of time. Let us also note that there is the surface $X = X_0(\tau)$, $X_0 = -D\tau^2$, where dispersion frequency shift compensates frequency shift caused by inhomogeneity, so eigen oscillations frequency is zero. The frequency of corresponding disturbance in form (2.1) is ω on this surface.

4.1. Dispersive resonant disturbances

(1) In this paragraph, we assume $A \ll |D|$. First, we examine the spatio-temporal structure of G for the case when the resonant disturbance is generated by the transversely localized large-scale mode (3.15). Let us denote the exponent in (3.15) by P and write it in the form $P = i\frac{2}{3} X u_c + iDu_c^3 (s^2 + \frac{1}{3} s^3) - \frac{1}{3} Au^3 + \gamma u_c + \gamma s u_c$, where, as above, $s = u/u_c - 1, u_c = (-X/D)^{1/2}$. It is assumed for u_c that $-X/D > 0$ and $u_c > 0$. The critical point u_c of the phase ϕ (as above, $\phi = \frac{1}{3} Du^3 + Xu$)) represents the point where dispersion and inhomogeneous frequency shifts compensate each other and the frequency of non-stationary eigen oscillations is 0. The point u_c is on

https://doi.org/10.1017/S002237781000022X Published online by Cambridge University Press

the integration interval if X is such that the inequality $0 \leqslant -X/D \leqslant \tau^2$ is fulfilled. We see that the phase ϕ and the part of P, resulting from non-stationarity of the driver $(\gamma u_c + \gamma s u_c)$, have scales of change (in the variable s) $(Du_c^3)^{-1/2}$ and $(\gamma u_c)^{-1}$, respectively. If $A = 0$, and $(Du_c)^{1/2} \gg \gamma$, *i.e.* X is in the region where

$$|X| / |D|^{1/3} \gg \left[\gamma / |D|^{1/3}\right]^4 \tag{4.2}$$

is met, the phase undergoes the most rapid change. If X is in the region where the inequality opposite to (4.2) is valid, the part of P resulting from non-stationarity of the driver changes most rapidly.

Let us first consider the case when $\gamma/|D|^{1/3} \ll 1$. In this case, in the region of X where the condition $|X|/|D|^{1/3} \gg 1$ is satisfied, the inequality (4.2) is also met. Change in the absorption part, if $A \neq 0$, may be neglected in the region (3.8). If X is such that u_c is on the integration interval, then changing P by its approximation near u_c,

$$P = i\frac{2}{3}Xu_c + iDu_c^3\, s^2 - \frac{1}{3}Au_c^3 + \gamma u_c, \tag{4.3}$$

and integrating (3.15) with account for equality $\int_{-\infty}^{\infty} \exp[\pm i\lambda^2] d\lambda = \sqrt{\pi} \exp[\pm i\frac{\pi}{4}]$, we get a quasi-stationary small-scale wave

$$G_{QS} = \exp\left[\gamma / D^{1/3}\left(|X/|D|^{1/3}|^{1/2} - |X_0/|D|^{1/3}|^{1/2}\right)\right] G_S, \tag{4.4}$$

where G_S is the stationary wave (3.10). The quasi-stationary behavior of G results from the fact that the main contribution to (3.15) is made by the vicinity of the critical point in which the frequency of non-stationary eigen oscillations G_0 is 0. According to (4.4), G has small-scale spatial structure of the wave (3.10). Due to the factor $\exp[\gamma/D^{1/3}(|X/|D|^{1/3}|^{1/2} - |X_0/|D|^{1/3}|^{1/2})]$, amplitude of the wave leaving the resonant surface decays as the driver decay. The wave propagates in the region where condition $\mathrm{sign}X = -\mathrm{sign}D$ is fulfilled. Thus, the inertial wave propagates in the region $X < 0$, and the kinetic one propagates in the region $X > 0$.

As has been shown above, G represents superposition of induced and eigen oscillations (4.1) quite far from the resonant surface. In the case (3.14), we have

$$G_I = -\frac{1}{X}\exp[-\gamma\tau], G_E = \frac{1}{X}G_0.$$

On the resonant surface side of the small-scale wave propagation, G is the superposition of induced and eigen oscillations if X is such that u_c is not on the integration interval, *i.e.* $-X/D > \tau^2$.

Thus, we can determine frontal line $X = X_F(\tau)$. We have $X_F(\tau) = X_0(\tau)$. Behind the frontal line, G has the form of a wave G_{QS} (4.4), and in front of it, represents superposition of eigen and induced oscillations. The front velocity, as well as the energy density flux q_S (2.11), is directed from the resonant surface independent of a dispersion coefficient sign. The front velocity coincides with the phase velocity of eigen oscillations G_0 : $V_F = -D\tau$. Directions of the phase velocity of small-scale wave G_{QS} and front velocity coincide at $D < 0$, and are opposite at $D > 0$. Structure of the front, *i.e.* of the disturbance near the frontal line, can be described analytically.

https://doi.org/10.1017/S002237781000022X Published online by Cambridge University Press

Let us write (3.15) in the form

$$G = iu_c \exp\left[-\gamma\tau\right]\left[\int_{-1}^{0} \exp P\,ds + \int_{0}^{\tau/u_c-1} \exp P\,ds\right].$$

Using the expression (4.3) for P near u_c and taking into consideration smallness of the phase change scale ($Du_c^3 \gg 1$), we get

$$G_F = iu_c \exp[-\gamma\tau] \exp\left[i\frac{2}{3}Xu_c - \frac{1}{3}Au_c^3 + \gamma u_c\right]$$

$$\times\left[\int_{-\infty}^{0} \exp\left[iDu_c^3\ s^2\right] ds + \int_{0}^{\tau/u_c-1} \exp\left[iDu_c^3\ s^2\right] ds\right].$$

It is clear that G is equal G_F not only near frontal line but at every place where quasi-stationary small-scale wave dominates in disturbance, *i.e.* on the front and behind it. Let us denote

$$\eta(X,\tau) = \tau/u_c - 1 = (X_0(\tau)/X)^{1/2} - 1$$

and

$$L(X,\tau) = \exp\left[-il_{\pm}\frac{\pi}{4}\right]\left|X/|D|^{1/3}\right|^{3/4}\eta.$$

Then

$$G_F = \frac{1}{2}g_F G_{QS}, \quad g_F = 1 + \mathtt{erf}\,(L). \tag{4.5}$$

Let us denote value of G on the frontal line by G_{F0}. To calculate G_{F0}, we let τ be equal to u_c. We obtain

$$G_{F0}(\tau) = \frac{1}{2}G_S\left(X_0(\tau)\right) = |D|^{-1/3}\,\frac{1}{2}\,i\pi^{1/2}$$

$$\times \exp\left[i\mathtt{sign}(D)\frac{\pi}{4}\right]\left(|D|^{1/3}\tau\right)^{-1/2} \exp\left[-\frac{2}{3}iD\tau^3\right] \exp\left[-\frac{1}{3}A\tau^3\right]. \tag{4.6}$$

According to (4.5) the front passage time $\Delta\tau_{F0}$ through the fixed point X decreases, if we move X away from the resonant surface: $\Delta\tau_{F0}(X) = |D|^{-1/3}|X/|D|^{1/3}|^{-1/4}$, and the front width ΔX_{F0} increases with time: $\Delta X_{F0}(\tau) = 2|D|^{1/3}(|D|^{1/3}\tau)^{1/2}$.

If $\gamma = 0$, the envelope of the small-scale wave is determined only by $g_w(X,\tau)$:

$$g_w = \frac{1}{2}i\pi^{1/2}\left|X/|D|^{1/3}\right|^{-1/4}(1 + erf(L)) \exp\left[-\frac{1}{3}\frac{A}{D}\left|X/|D|^{1/3}\right|^{3/2}\right],$$

and we have

$$G = G_W, G_W = |D|^{-1/3}\ g_w \exp\left[isign(D)\left(-\frac{2}{3}\left|X/|D|^{1/3}\right|^{3/2} + \frac{\pi}{4}\right)\right].$$

Figure 1 shows formation of the wave G_F for $\gamma/D = 0.3$, $A = 0$. Curves in Fig. 1 and subsequent figures were obtained by numerical calculation of the integral (3.12). In each case, analytical curves coincide with those calculated numerically.

Let us now consider the case when $\gamma \gg |D|^{1/3}$. If $\gamma \gg |D|^{1/3}$, there is a large region of X values at which the condition opposite to (4.2) is met:

$$|X|/\gamma \ll \left(\gamma/|D|^{1/3}\right)^3. \tag{4.7}$$

https://doi.org/10.1017/S002237781000022X Published online by Cambridge University Press

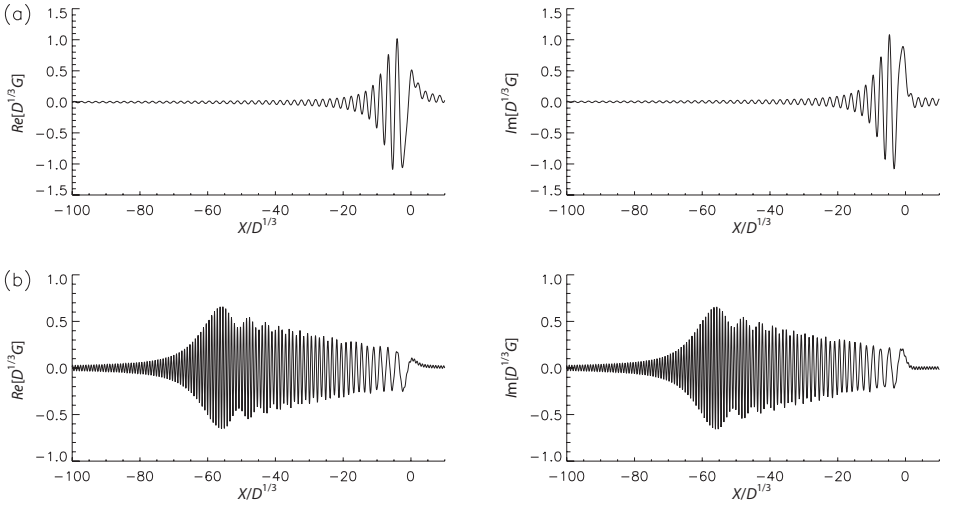


Figure 1. Formation of the quasi-stationary wave in the case of localized large-scale wave for $\gamma/D^{1/3} = 0.3, A = 0$: (a) $\tau D^{1/3} = 3$, (b) $\tau D^{1/3} = 8$.

At this X, the exponent P as function of s varies with the scale $(\gamma u_c)^{-1}$ in the vicinity of the point u_c. For X of this region, we have $P = i\frac{2}{3}Xu_c - \frac{1}{3}Au_c^3 + \gamma u_c + \gamma u_c s$ near u_c. This implies that the presence of the critical point in this case is insignificant, and the value of integral (3.15) is determined by integrals near end points of the integration interval. At $\gamma\tau \gg 1$, induced oscillations may be ignored because the integrand decreases dramatically to $u = 0$. Setting $P = i(D\tau^2 + X - i\gamma)(u - \tau) - \frac{1}{3}A\tau^3$ near $u = \tau$, we get at $\gamma\tau \gg 1$

$$G_{ND} = \frac{1}{\gamma}\frac{1}{(X - X_0(\tau))/\gamma - i}G_0, \tag{4.8}$$

for X values satisfying the inequality (4.7). According to (4.8), G represents a packet of propagating eigen non-stationary oscillations ("non-stationary packet"). Let us define center of the packet X_c as a surface where $|G|$ takes its maximum value. We have $X_c = X_0(\tau)$. Thus the packet propagates at velocity of the quasi-stationary small-scale wave front: $V_c = -D\tau$. According to (4.8), the packet width ΔX_p is a constant value ($\Delta X_p \sim \gamma$) and $\max|G| \sim \frac{1}{\gamma}$; *i.e.* it does not change its form when propagating. Oscillation frequency in the packet is a function of X and τ. It varies linearly over the region of packet localization, and there are variable frequency oscillations at a selected point through which the packet passes. With distance away, the packet leaves the region where (4.7) is met and comes to the range of X values satisfying (4.2). In this region, the disturbance structure is determined by the integral near the critical point, therefore the packet becomes asymmetric, taking the leading edge. As follows from (4.2), this transformation occurs at $\tau|D|^{1/3} \sim [\gamma/|D|^{1/3}]^2$. The absorption should be sufficiently small for the non-stationary oscillations (4.8) not to damp in the range of X values satisfying (4.2): $A/|D| \ll (|D|^{1/3}/\gamma)^{3/2}$.

Figure 2 shows the spatio-temporal evolution of the non-stationary wave packet (4.8) at $A = 0$, $\gamma/D^{1/3} = 8$. In Fig. 2(a), form of the packet is symmetric about

https://doi.org/10.1017/S002237781000022X Published online by Cambridge University Press

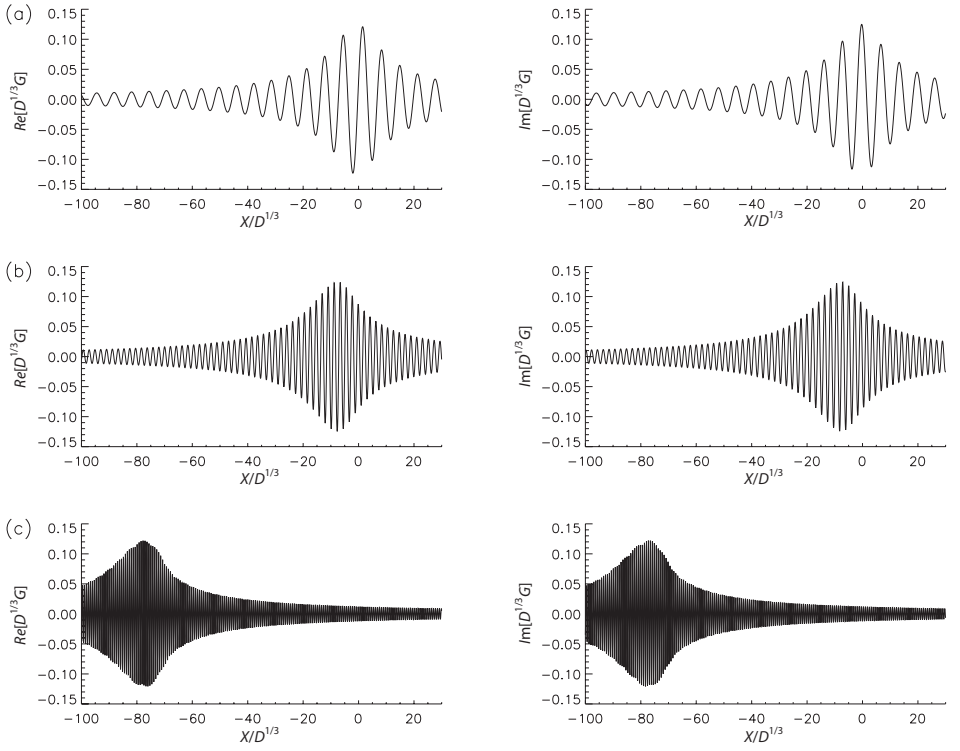


Figure 2. Evolution of the non-stationary packet in the case of localized large-scale wave for $\gamma/D^{1/3} = 8, A = 0$: (a) $\tau D^{1/3} = 1$, (b) $\tau D^{1/3} = 3$, (c)$\tau D^{1/3} = 9$.

its center; in Fig. 2(c) it is asymmetric because of transformation into a form of quasi-stationary packet.

(2) Let us study formation of G with quasi-stationary and non-stationary structures for the case when the resonant disturbance is generated by a transversely non-localized large-scale mode of finite duration. We assume, as in the previous case, $A \ll |D|$.

As is seen from above, the quasi-stationary wave is formed if the driver varies not too strongly and its scale of change is much larger than the scale of change of the phase near the critical point. It is clear that the quasi-stationary wave G_{S1} generated by the driver $f_1(\tau)$ has the form: $G_{S1}(X, D, \tau) = f_1(\tau - (-X/D)^{1/2})G_S(X, D, \tau)$, where G_S is the stationary wave (3.10). If the induced and the eigen oscillations are small as compared to G_{S1}, we have $G = G_{S1}$.

Let us concretize f_1 as $f_1 = 1$. In this case a quasi-stationary wave arises if the critical point is in the integration interval and the scale of change of the phase is smaller than the integration interval length. Consequently, we get (4.2) with replacement $\gamma \to \tau_1^{-1}$ as the condition for formation of quasi-stationary wave. Thus, when $\tau_1|D|^{1/3} \gg 1$, we obtain $G = G_W$ at $\tau \leqslant \tau_1$ in the region $1 \ll |X|/|D|^{1/3} < (|D|^{1/3}\tau)^2$, sign$X = -$sign$D$. At $\tau > \tau_1$, G represents a quasi-stationary packet with leading and trailing edges. The packet position in space can be easily found from the equations of the leading edge line ($X_{LF} = X_0(\tau)$) and that of the trailing edge line ($X_{TF0} = -D(\tau - \tau_1)^2$). Let us denote G on the leading and trailing

https://doi.org/10.1017/S002237781000022X Published online by Cambridge University Press

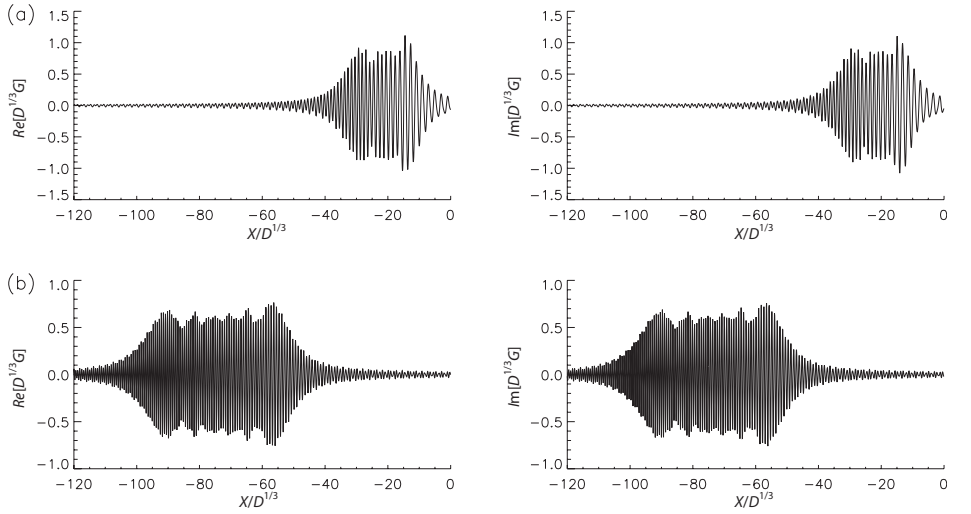


Figure 3. Evolution of the quasi-stationary packet in the case of the finite duration driver for $\tau_1 D^{1/3} = 3, A = 0$: (a) $\tau D^{1/3} = 6$, (b) $\tau D^{1/3} = 10$.

edge lines by G_{LF0} and G_{TF0}, respectively. We get equations similar to (4.6), *i.e.* $G_{LF0}(\tau) = \frac{1}{2} G_S(X_0(\tau)), G_{TF0}(\tau) = \frac{1}{2} G_S(X_{TF}(\tau))$. The quasi-stationary packet width is $L_p\ (\tau, \tau_1) = |D|\tau_1(2\tau - \tau_1)$; *i.e.* the packet expands linearly with time. Evolution of the quasi-stationary packet is demonstrated in Fig. 3 for $\tau_1 D^{1/3} = 3, A = 0$.

Note that in the case of sufficiently smooth driver, sharp edges of disturbance are absent. If we take bump-function f_b as f_1: $f_1 = f_b, f_b = \exp[1 - 1/(1 - (1 - \frac{u}{\tau_1})^2)]$, then we see that the integral near the critical point and the integral near $u = 0$ give $G = f_b/x + f_b(\tau - (-X/D)^{1/2})G_S$; we have $G = f_b(\tau - (-X/D)^{1/2})G_S$, when $\tau > \tau_1$.

To obtain G with non-stationary structure, we assume that τ_1 is much less than the dispersion time, *i.e.* $\tau_1 |D|^{1/3} \ll 1$. In this case, a non-stationary packet, retaining its features as long as it is in the region where X satisfies the inequality $|X|\tau_1 \ll (\tau_1 |D|^{1/3})^{-3}$, arises at $\tau \gg \tau_1$ (similarly to (4.7)). At $|X - X_0(\tau)| \ll \tau_1^{-1}$, the exponential factor change in (3.16) may be neglected, and we get

$$G = G_M, \qquad G_M = iG_0 \int_0^{\tau_1} f_1(\tau)\, d\tau. \tag{4.9}$$

If $f_1 = 1$, we have $G_M = i\tau_1 G_0$. To find G in the region $|X - X_0(\tau)| \gg \tau_1^{-1}$ it is sufficient to take integrals near end points. Thus we obtain

$$G = \frac{1}{[X - X_0(\tau)]} G_0 \left[1 - \exp\left[-i(X - X_0(\tau))\tau_1\right]\right]. \tag{4.10}$$

We see that not only the main packet G_M but also the additional packets appear. According to (4.10) there is splitting of the frequencies of the main packet G_M and the packets (4.10) and this splitting increases in time. The entire structure moves at the velocity $V_F = -D\tau$. Maximum of $|G|$ is $\sim \tau_1$ and width is $\sim \tau_1^{-1}$. When the packet transfers to the range of sufficiently large X values ($|X| \gg (\tau_1 |D|^{1/3})^{-3}$), the scale of phase change gets smaller than τ_1, and the packet G_M loses its non-stationary character.

https://doi.org/10.1017/S002237781000022X Published online by Cambridge University Press

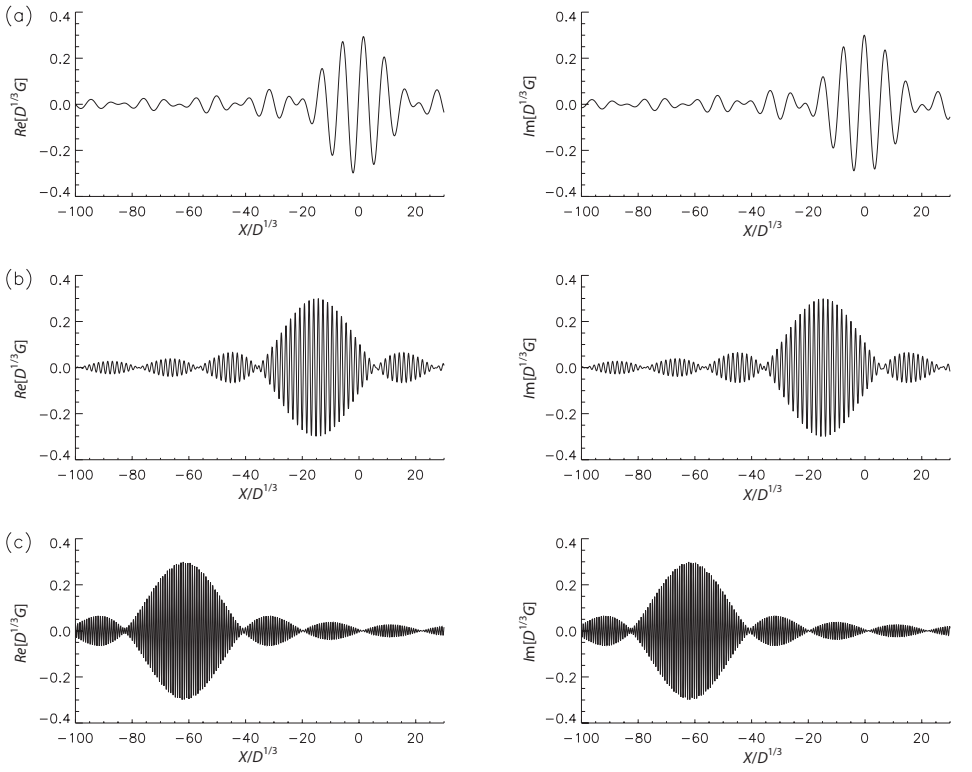


Figure 4. Evolution of the non-stationary packet in the case of the finite duration driver for $\tau_1 D^{1/3} = 0.3, A = 0$: (a) $\tau D^{1/3} = 1$, (b) $\tau D^{1/3} = 4$, (c) $\tau D^{1/3} = 8$.

The main packet (4.9) and accompanying packet (4.10) for $f_1(\tau) = 1$ are shown in Fig. 4 at $\tau_1 D^{1/3} = 0.3, A = 0$.

(3) The longitudinal electric field of dispersive Alfven waves, well known from the analytical stationary solution and non-stationary numerical calculations, has long been connected to small-scale structure of fluxes of accelerated charged particles precipitated into the ionosphere (Goertz & Boswell 1979; Stasiewicz et al. 2000). Considering energy density fluxe q_S (2.11) as dimensionless Poynting vector, *i.e.* supposing $q_S = -\frac{c}{4\pi} E_z B_y / (\omega B_0^2 / k_z)$, we get for the longitudinal electric field amplitude:

$$e_z = -\frac{\omega B_0}{c k_z} i d \partial_\chi h_y^{(-1)} \text{ or } e_z / \left[\left(\frac{\omega B_0}{c k_z} \right) \left(2D \left(\left| \left(\partial \chi U_a^2 \right) (x_0) \right| \right)^{-1} F_0 \frac{k_y}{k_z} \right) \right] = -i \partial_X G.$$

According to (4.5) and (4.8) we have

$$\partial_X G_F = i |D|^{-1/3} |X/|D|^{1/3}|^{1/2} G_F, \partial_X G_{ND} = i \tau G_{ND}.$$

We see that the longitudinal electric field increases as the resonant disturbance moves away from the resonance surface. Its amplitude takes maximal value on the front of the quasi-stationary wave (E_F) and in the center of the non-stationary packet (E_c). We can see from (4.5) and (4.8) that $E_F \propto \tau^{1/2}, E_c \propto \tau$.

https://doi.org/10.1017/S002237781000022X Published online by Cambridge University Press

(4) Let us summarize the picture of evolution of the dispersive resonance disturbance from the above formulae.

(i) If the driver duration and time scale of its change are far in excess of the dispersion time, a resonance Alfven disturbance is formed with large-scale wave frequency and spatio-temporal envelope defined by temporal behavior of the large-scale wave amplitude. Such quasi-stationary disturbance propagates as a wave with leading edge, if the driver amplitude is not zero at the initial instant of time; the front travels with constant acceleration. The front spreads out in space. Disturbance before the front represents a superposition of induced oscillations and eigen oscillations with variable frequency. After the ceasing of the driver, such a disturbance is like a spreading-in-space packet.

(ii) If the dispersion time far exceeds the driver duration, a symmetric-about-the-center, non-spreading packet of eigen oscillations with time-variable frequency is formed first. Such non-stationary packet goes away from the resonant surface with the velocity of the quasi-stationary wave front. When propagating, this packet transforms into the quasi-stationary one if absorption is sufficiently small.

In the case of the quasi-monochromatic disturbance, amplitude is defined by the dispersion time, while it is defined by the driver duration in the case of the non-stationary packet. Disturbance propagates from the resonant surface upwards or downwards of the local Alfven frequency depending on whether dispersion is inertial or kinetic.

4.2. Absorbed resonant disturbances

In this paragraph, we assume that $A \gg |D|$. When the absorption coefficient far exceeds the dispersion one, the analysis of (3.12) can be reduced to the Laplace method for the integral with a real large parameter over the real interval. This variant of the Laplace method can be applied in presence of the factor of the form $\exp[-Zr(v)]$ (where $Z > 0, r(v)$ is a real function) in the integrand of the integral over real variable. In this case, approximate integral values as $Z \to \infty$ are reduced to the integral near the point with the minimum of function $p(v)$.

(1) Let us consider the case when the resonant disturbance is generated by transversely localized large-scale mode (3.15). Denote $\tau_m = (\gamma/A)^{1/2}$. The real part of P has the local maximum at $u = \tau_m$. At $\tau = \tau_m$ decrements due to absorption $(A\tau^2)$ and the driver's non-stationarity (γ) are equal. Note that τ_m is greater than both the time of the driver decay and the absorption time.

Let us introduce the notation $u = \tau_m(1+w)$ and write the exponent P in the form

$$P = \frac{2}{3}A\tau_m^3 - A\tau_m^3\left(w^2 + \frac{1}{3}w^3\right) + iX\tau_m(1+w) + \frac{1}{3}iD\tau_m^3(1+w)^3.$$

In the case $\gamma\tau_m \ll 1$, *i.e.* at $\gamma/A^{1/3} \ll 1$, the presence of τ_m may be neglected, because τ_m is close to 0 and $\exp P_{u=\tau_m} \approx \exp P_{u=0}$. We may also put $\exp[i\frac{1}{3}Du^3] = 1$. Thus, we get

$$G = \exp[-\gamma\tau]\, G_A, \quad G_A = iA^{-1/3}\int_0^\infty \exp\left[-\frac{1}{3}v^3 + i\left(X/A^{1/3}\right)v\right] du \tag{4.11}$$

at $\tau \gg A^{-1/3}$.

According to (4.11), G has spatial structure of the stationary absorption solution G_A (*i.e.* the solution (3.6) with $D = 0$) and its amplitude varies following driver

https://doi.org/10.1017/S002237781000022X Published online by Cambridge University Press

amplitude variations. Solution G_A corresponds to the stationary absorbed disturbance; it studied, for instance, in Ruderman et al. (1995). The width of the region where the disturbance is localized and the spatial scale of the disturbance are of the order of $A^{1/3}$.

In the case $\gamma/A^{1/3} \gg 1$, we have $\exp(\frac{2}{3}A\tau_m^3) \gg 1$, therefore presence of τ_m may be significant. While $\tau < \tau_m$, the point $u = \tau_m$ is not on the interval of integration, hence only the contributions of the integrals near the end points should be considered. As $\exp[-\frac{1}{3}Au^3 + \gamma u]$ decreases with the scale γ^{-1} to 0, the contribution of the lower limit may be neglected at $\tau\gamma \gg 1$. As $P = i\frac{1}{3}D\tau^3 - \frac{1}{3}A\tau^3 + iXu + \gamma u$ near $u = \tau$ at $\tau \ll \tau_m$, we obtain

$$G = G_{NA}, \quad G_{NA} = \frac{1}{\gamma}\frac{1}{X/\gamma - i}G_0, \tag{4.12}$$

when $1 \ll \tau\gamma \ll \gamma\tau_m$.

The maximum point $u = \tau_m$ appears on the integration interval at $\tau \geqslant \tau_m$. If $X\tau_m \ll (A\tau_m^3)^{1/2}$ (*i.e.* $X \ll \gamma$) and $D\tau_m^3 \ll (A\tau_m^3)^{1/2}$ (*i.e.* $D/A \ll (\gamma/A^{1/3})^{-3/4}$), change in the phase near the maximum point may be neglected. Hence, we have $P = \frac{2}{3}A\tau_m^3 - A\tau_m^3 w^2 + iX\tau_m + \frac{1}{3}iD\tau_m^3$. As $\gamma/A^{1/3} \gg 1$ is assumed, we can calculate contribution of the vicinity of τ_m to the integral in (3.15) as $\int_{-\infty}^{\infty}\tau_m \exp P\,dw$ and $\int_{-\infty}^{0}\tau_m \exp P\,dw$ at $\tau - \tau_m \gg (A\tau_m^3)^{-1/2}$ and $\tau = \tau_m$, correspondingly.

Denoting

$$G_{A1}(X, A, \tau) = i\pi^{1/2}\gamma^{-1}\left(\frac{\gamma}{A^{1/3}}\right)^{3/4} \times \exp[-\gamma\tau]\exp\left[\frac{2}{3}\,\gamma\tau_m\right]\exp[iX\tau_m]\exp\left[\frac{1}{3}iD\tau_m^3\right], \tag{4.13}$$

we get $G = G_{A1}(X, \tau)$ and $G = \frac{1}{2}G_{A1}(X, \tau_m)$ at $\tau - \tau_m \gg (\gamma/A^{1/3})^{-3/4}$ and $\tau = \tau_m$, correspondingly. The quasi-stationary disturbance (4.13) decays as a whole with the driver decrement, retaining the spatial structure of the non-stationary eigen oscillations (4.12) at $\tau = \tau_m$. The spatial scale is τ_m^{-1}; *i.e.* it is smaller than that in the quasi-stationary case. A similar structure was found for the case $\gamma/A^{1/3} \gg 1$ by numerical calculation in studies of decaying normal modes by Ruderman et al. (1995), who concluded that resonant disturbance amplitude increases when $\gamma/A^{1/3}$ decreases. Considering the resonant disturbance as a result of evolution allows us to compare amplitudes in cases (4.13) and (4.11). Choosing identical initial amplitudes of drivers and coefficient A but different values of γ : $\gamma_1/A^{1/3} \ll 1$ and $\gamma_2/A^{1/3} \gg 1$, it easy to see that the resonant disturbance amplitude with γ_1 exceeds that with γ_2. The resonant disturbance amplitude with structure (4.13) is lower because it arises when the driver dramatically decays.

Figures 5 and 6 show G for $\gamma/A^{1/3} = 0.3$ and $\gamma/A^{1/3} = 4$. Curves corresponding to two larger values of $\tau A^{1/3}$ show stationary spatial structures (4.11) (Fig. 5) and (4.13) (Fig. 6), respectively.

(2) Let us consider the case when the resonant disturbance is generated by the driver of finite duration with $\tau_1 \ll A^{-1/3}$.

If $\tau \ll (A\tau_1)^{1/2}$ and $|X| \ll \tau_1^{-1}$, the exponential factor change in (3.16) may be neglected, then we get the decaying eigen oscillations (4.9). If $f_1 = 1$ we have $G_M = i\tau_1 G_0$. To find G at $|X| \gg \tau_1^{-1}$ for any τ, and G at $\tau \gg \tau_1(A^{1/3}\tau_1)^{3/2}$ for any X,

https://doi.org/10.1017/S002237781000022X Published online by Cambridge University Press

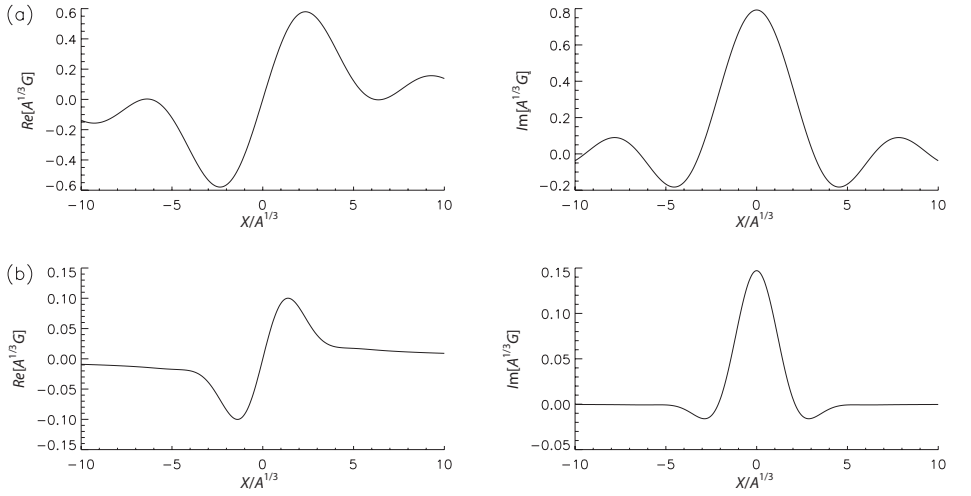


Figure 5. Formation of the quasi-stationary absorbable disturbance in case of localized large-scale wave for $\gamma/A^{1/3} = 0.3$, $D = 0$: (a) $\tau A^{1/3} = 1$, (b) $\tau A^{1/3} = 8$.

it is sufficient to take integrals near end points. Then we get

$$G = \frac{i}{-A\tau^2 + iX} G_0[1 - \exp[-iX\tau_1 + A\tau^2\tau_1]].$$

Thus the amplitude of the non-stationary disturbance is of the order of τ_1. The disturbance is localized on the scale τ_1^{-1} near the resonance surface, its decay is defined by the absorption time.

5. Conclusion

Using analytical solution to the evolution resonance equation taking account of dispersion and absorption of Alfven waves, we show that the disturbance evolution in the thin resonance layer can be studied (ignoring minor details of evolution at the initial short stage of the quasi-stationary conversion regime establishment) as evolution of the disturbance generated by certain drivers. In order to describe evolution of resonant disturbance in the case of the transversely localized large-scale mode, we prescribe function exponentially decreasing from the initial moment of time as a driver in the resonance layer. Function of finite duration is chosen as driver in the case of the non-localized large-scale wave.

It is shown that character of the resonant disturbance evolution is determined by the ratio of resonance detuning factors. Each resonance detuning factor (the Alfven wave dispersion, Alfven disturbance absorption, driver non-stationarity) brings its length into the resonance disturbance (small in comparison with each of driver wavelengths) and its time (large in comparison with the driver period). Each spatial length is inversely proportional to its time.

In this paper, we have shown that if the dispersion time is less than the absorption one, then formation of propagating small-scale Alfven disturbances of two types is possible: the first type is the monochromatic disturbance with spatio-temporal envelope (‘quasi-stationary disturbance’), the second one is eigen oscillations with the

https://doi.org/10.1017/S002237781000022X Published online by Cambridge University Press

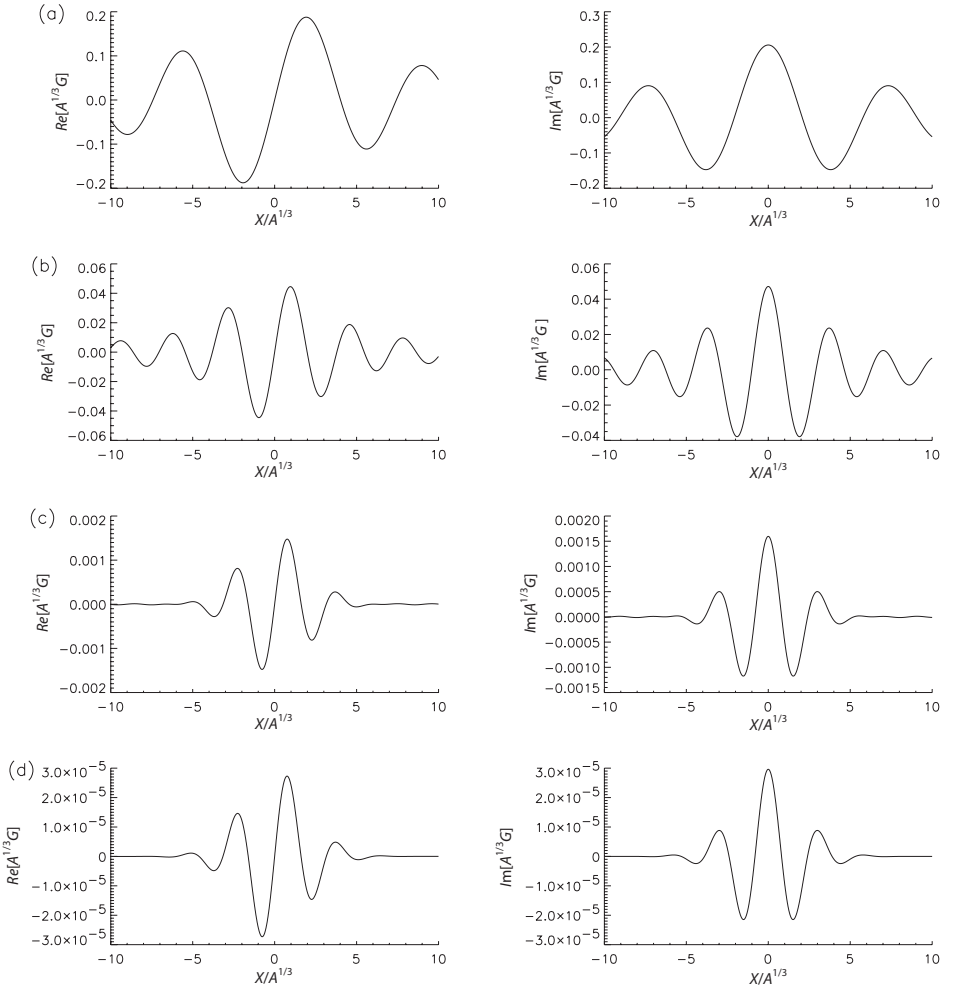


Figure 6. Evolution of small-scale absorbable disturbance in case of localized large-scale wave for $\gamma/A^{1/3} = 4, D = 0$: (a) $\tau A^{1/3} = 1$, (b) $\tau A^{1/3} = 2$, (c) $\tau A^{1/3} = 3$, (d)$\tau A^{1/3} = 4$.

frequency changing in time and space ('non-stationary disturbance'). Disturbance propagates from the resonant surface in the direction of decrease or increase in the local Alfven frequency, depending on whether the kinetic or inertial dispersion occurs.

Quasi-stationary disturbance is formed when the driver duration is much larger than the dispersion time; *e.g.* the time of the damping of the large-scale mode caused by conversion into the resonant disturbance is much larger than the dispersion time. Such a resonant disturbance has the driver frequency and spatio-temporal envelope defined by temporal behavior of the driver. For the case of the non-zero initial amplitude of the driver, such a disturbance is shown to propagate as the wave, having the front which is in uniformly accelerated motion. Disturbance preceding the front is not quasi-stationary but it is a superposition of eigen oscillations with variable frequency and induced monochromatic oscillations; the front spreads

https://doi.org/10.1017/S002237781000022X Published online by Cambridge University Press

in space. The quasi-stationary resonant disturbance amplitude is proportional to the dispersion time. When the driver ceases, this disturbance behaves as a packet spreading in space.

If the driver duration is much smaller than the dispersion time, the non-stationary disturbance is generated in the form of a non-spreading packet of eigen oscillations with variable frequency. This packet is symmetric about its center. It moves away from the resonant surface at the velocity of the monochromatic wave front. Amplitude is proportional to the driver time (in the case of the transversally localized large-scale mode, the driver time is inversely proportional to the decrement). Structure of this packet transforms into structure of the quasi-monochromatic packet with distance away from the resonant surface. Eigen oscillations are damped with decrement increasing with time, which is small in comparison with the frequency shift caused by the dispersion. Their spatial scale at a given point of space undergoes refinement with time, unlike quasi-stationary oscillations whose spatial scale remains unchanged at a given point of space. However, the farther is the point from the resonance surface, the smaller is the spatial scale of the quasi-stationary disturbance. Refinement of spatial scale with time leads to increasing of longitudinal electric field on the front of the quasi-stationary disturbance and in the center of the non-stationary packet with time.

We also give analytical descriptions of the resonant disturbance evolution for the case when the absorption time is smaller than the dispersion one. In this case, the disturbance localized near the resonant surface is formed. If the driver time is much larger than the absorption time scale, the resonant disturbance with spatial structure of the monochromatic disturbance is formed; its amplitude varies with time following the driver amplitude. In the case of the driver exponentially decaying with time, which is smaller than the absorption one, eigen oscillations with the local Alfven frequency and absorption decrement increasing with time are formed initially. Space refinement inherent in non-stationary eigen oscillations stops when the driver and absorption decrements of eigen oscillations increasing with time become equal. As a result, disturbance becomes quasi-stationary at the stage of its disappearance and decays with the driver decrement, keeping structure of eigen oscillations that corresponds to this instant of time.

Appendix A

In order to derive equations of disturbance in the one-dimensionally resonance layer and formulae of the large-scale disturbance matching through the resonance layer, we use linearized equations of one-fluid MHD with pressure as initial ones:

$$\begin{aligned}
\partial_t \mathbf{B}_\perp &= B_0 \partial_z \mathbf{v}_\perp, \\
div\mathbf{B} &= 0, \\
m_i n_0 \partial_t \mathbf{v}_\perp &= -\nabla_\perp P_t + \frac{1}{4\pi} B_0 \partial_z \mathbf{B}_\perp, \quad P_t = P + \frac{1}{4\pi} B_0 B_z, \\
m_i n_0 \partial_t \mathbf{v}_z &= -\partial_z P + \frac{1}{4\pi} (\mathbf{B}_\perp \nabla) \mathbf{B}_0, \\
\partial_t n + \nabla \cdot n_0 \mathbf{v} &= 0, \\
\partial_t P + (\mathbf{v}\nabla) P_0 + \gamma P_0 div\mathbf{v} &= 0.
\end{aligned} \tag{A 1}$$

https://doi.org/10.1017/S002237781000022X Published online by Cambridge University Press

Unperturbed pressure and magnetic field are connected by $\partial_x(P_0 + \frac{B_0^2}{8\pi}) = 0$. Sign $\perp$ denotes the vector component perpendicular to z-axis. Assuming (2.2) and (2.3), we get

$$\widehat{L}_a^{(1)} B_y^{(-1)}/B_0(0) = V_a^2(0)\partial_z\partial_y\left[4\pi P_t^{(0)}/B_0^2(0)\right],$$

where

$$\widehat{L}_a = -\partial_{tt}^2 + V_a^2\partial_{zz}^2 \tag{A 2}$$

from the first three equations (A 1) for the disturbance (2.1) in the resonance layer. The superscript denotes order of magnitude in power of Δ. Using

$$\partial_{tt}^2 = \omega^2\partial_{\theta\theta}^2 - 2\omega\partial_T\partial_\theta + O(\Delta^2), \quad \left(\partial_x V_a^2\right)(x_0) \sim \Delta^{(0)}, \quad (x - x_0) \sim \Delta, \tag{A 3}$$

we derive resonance equation in the form

$$\left[2\omega\partial_T\partial_\theta + \left(\partial_x V_a^2(x_0)\right)(x - x_0)\,\partial_{zz}^2\right] B_y^{(-1)}(x, T, \theta)/B_0(x_0)$$

$$= V_a^2(x_0)\partial_z\partial_y\left[4\pi P_t^{(0)}(T, \theta)/B_0^2(x_0)\right].$$

Note, that (A 1) gives

$$B_y^{(-1)}/B_0(0) = -v_y^{(-1)}/V_a(x_0), B_x^{(0)}/B_0(0) = -v_x^{(0)}/V_a(x_0). \tag{A 4}$$

Appendix B

To get a non-stationary resonance equation with dispersion and collisionless absorption, we use the kinetic dispersion equation. For low-frequency oscillations ($\omega/\omega_i \ll 1$) the dispersion equation (Akhiezer et al.1974) is

$$\omega^2 - V_a^2 k_z^2\left(1 - K\ k_\perp^2\right) = 0, \tag{B 1}$$

$$K = -\rho_s^2/\left[1 + i\sqrt{\pi}\frac{\omega}{\sqrt{2}k_z v_e} w\left(\frac{\omega}{\sqrt{2}k_z v_e}\right)\right] + \frac{3}{4}\rho_i^2, \rho_s = \frac{1}{\omega_i}\left(\frac{T_e}{m_i}\right)^{1/2},$$

$$\rho_i = \frac{1}{\omega_i}\left(\frac{T_i}{m_i}\right)^{1/2}, \ v_e = \left(\frac{T_e}{m_e}\right)^{1/2},$$

where w is the plasma dispersion function: $w(z) = e^{-z^2/2} erfc(-iz), erfc$ is the complementary error function (Abramovitz and Stegan 1970; Akhiezer et al. 1974). Given $\frac{\omega}{k_z} \gg v_e$ and $\frac{\omega}{k_z} \ll v_e$, we have $\mathtt{Re}K = \frac{c^2}{\omega_{pe}^2}$ and $\mathtt{Re}K = -(\rho_s^2 + \frac{3}{4}\rho_i^2)$, respectively. In the first case, the kinetic dispersion equation (B 1) coincides with the dispersion equation of two-fluid cold plasma MHD (Swanson 1975) and describes inertial Alfven waves. In the second case, the kinetic dispersion (B 1) coincides with the dispersion equation of two-fluid plasma MHD with finite pressure, except for the coefficient $\frac{3}{4}$ (Hasegawa and Chen 1976), and describes kinetic Alfven waves. Imaginary part of K describes collisionless absorption of Alfven waves. Let us designate $d = k_z^2 \mathtt{Re}K(x_0)$ and $a = k_z^2 \mathtt{Im}K(x_0)$. $\mathtt{Re}K$ may be positive or negative, $\mathtt{Im}K$ takes only positive values.

We can complete the operator $\widehat{L}_a$ (A 2) by an operator accounting for dispersion and absorption from the dispersion equation for the homogeneous case (B 1), as the scale of inhomogeneity is assumed to be larger in comparison with the scale of the

https://doi.org/10.1017/S002237781000022X Published online by Cambridge University Press

resonance disturbance ((A 3)). As according to (2.2) and (2.3) $k_x \sim \Delta^{-1}$ and $k_y \sim \Delta^0$, we change $k_\perp^2$ to $-\partial_{xx}^2$. According to (2.1), factor i means ∂_θ, so K is replaced by $\widehat{K} = ReK + ImK\,\partial_\theta$. As a result, operator $\widehat{L}_a$ is changed to $\widehat{L}_a = -\partial_t\partial_t + V_a^2\partial_z\partial_z(1+\widehat{K}\partial_{xx}^2)$ and the resonance equation takes the form (2.6).

Construction of differential operator from the dispersion equation may be justified when the kinetic and two-fluid MHD tensors of dielectric permeability coincide, *i.e.* in the case of cold plasma. Consideration for the collisionless absorption and dispersion coefficients for kinetic waves is, in the framework of equations (2.4)–(2.6), of model character.

In the case of two-fluid MHD, given $\omega/\omega_i \ll 1$, the Hall current can be neglected in the sum of equations of motion of electrons and ions. Then we get an equation of motion where pressure P is replaced by the sum of ion and electron pressures. Thus, (2.4) is valid for the two-fluid MHD and $P_t^{(0)}$ does not depend on x.

Appendix C

In a particular case, $d = 0$, (2.6) coincides with the resonance equation of the one-fluid dissipative MHD, when instead of (A 1) we have

$$\partial_t \mathbf{B}_\perp = (\mathbf{B}_0\nabla)\,\mathbf{v}_\perp + \mu\nabla^2\mathbf{B}_\perp,$$

$$\partial_t \mathbf{v}_\perp = \frac{1}{m_i n_0}\left[\frac{1}{4\pi}(\mathbf{B}_0\nabla)\,\mathbf{B}_\perp - \nabla_\perp P_t\right] + \nu\nabla^2\mathbf{v}_\perp, \tag{C 1}$$

where μ is the coefficient of resistivity and ν is the coefficient of viscosity. When adding the condition $\mu\nabla^2 \sim \nu\nabla^2 \sim \Delta$ to conditions (2.2), (2.3), and (A 3) in the resonance layer for the disturbance of form (2.1), we derive (2.4), (2.5), and (2.6) with $d = 0$ and $a = [\nu+\mu]\,\frac{k_z^2}{\omega}$, from (C 1). It is clear that the two-fluid visco-resistive MHD gives (2.6) with dispersion coefficient for kinetic or inertial Alfven waves and the absorption coefficient $a = [\nu+\mu]\,\frac{k_z^2}{\omega}$.

Appendix D

For monochromatic wave with frequency ω we have in variables ψ and $\boldsymbol{h}_\perp$ (2.7):

$$\partial_{\chi\chi}^2\psi - \frac{\partial_\xi\left(qB_0^2\right)}{qB_0^2}\partial_\chi\psi + \left[U_a^{-2} - 1 - \frac{k_y^2}{k_z^2} - \frac{U_a^{-2}-1}{U_a^2U_S^{-2} - U_a^2 + 1}\right]\psi = 0, \tag{D 1}$$

where $U_S^2 = \frac{\gamma P_0}{m_i n_0}\frac{k_z^2}{\omega^2}$, and

$$h_x = i\frac{B_0}{B_0(x_0)}\frac{\partial_\chi\psi}{\left(1-U_a^2\right)}. \tag{D 2}$$

We can see that expansion for ψ by the Frobenius method near the resonant surface (*i.e.* when $|\chi| \to 0$) is identical to that for h_z in the cold plasma case (Southwood 1974):

$$\psi = A\left[\frac{1}{2}\frac{k_y^2}{k_z^2}\chi^2\right] + B\left[1 + \frac{1}{2}\frac{k_y^2}{k_z^2}\chi^2\ln\chi\right]. \tag{D 3}$$

https://doi.org/10.1017/S002237781000022X Published online by Cambridge University Press

If dispersion and dissipation are not taken into account in the resonance layer, the disturbance is described by (D 1) everywhere except for the resonant surface. A branch of logarithm should be chosen in (D 3) for matching of the monochromatic disturbance. For this purpose, we may add a small, positive, imaginary addition to frequency, corresponding to the increase in disturbance from $t = -\infty$, similarly to the Landau bypass rule for the plasma resonance. Then the singular point is shifted from the real axis to the complex region and we obtain $\ln(-|\chi|) = \ln|\chi| - i\pi\mathrm{sign}(\partial_x V_a(x_0))\cdot\mathrm{sign}\omega$.

Let us rewrite (D 3) in the form

$$\psi = A_{\pm}\left[\frac{1}{2}\frac{k_y^2}{k_z^2}\chi^2\right] + B_{\pm}\left[1 + \frac{1}{2}\frac{k_y^2}{k_z^2}\chi^2\ln|\chi|\right]. \tag{D 4}$$

The '+' and '−' signs refer to regions $\chi > 0$ and $\chi < 0$, respectively. Argument of the logarithm is included in the part of the solution with the coefficient $A_{\pm}$. We obtain the following matching formulae:

$$B_+ = B_- = B, \tag{D 5}$$

and assuming $\partial_x U_a^2(x_0) < 0, \omega > 0$,

$$A_+ - A_- = -i\pi B. \tag{D 6}$$

If disturbance assumed to be everywhere in the form of (2.1) with $\partial_T \sim \Delta$, it is described by (D 1) at $|\chi| \gg \Delta$. We have when $|\chi| \to 0, |\chi| \gg \Delta$ instead of (D 4)

$$\psi = A_{\pm}(\tau)\left[\frac{1}{2}\frac{k_y^2}{k_z^2}\chi^2\right] + B_{\pm}(\tau)\left[1 + \frac{1}{2}\frac{k_y^2}{k_z^2}\chi^2\ln|\chi|\right]. \tag{D 7}$$

Note that according to (D 7) the scale of ψ is $\frac{k_z}{k_y}$ and the condition of applicability (D 7) is $|\chi| \ll \frac{k_z}{k_y}$, but because another scales can be induced, for instance, by inhomogeneity structure or a turning point, we will write the condition of applicability of (D 7) as $|\chi| \ll L$.

If dispersion and dissipation are taken into consideration in the resonance layer (on the scale Δ), then matching is realized by the usage of the solution (3.12) for the resonance layer, and equations of matching take the following form:

$$B_+(\tau) = B_-(\tau) = B(\tau),\ A_+(\tau) - A_-(\tau) = -i\pi B(\tau).$$

As $B(\tau) = \psi^{(0)}$ and $\psi^{(0)} = F_0 f(\tau)$, we have

$$B_+(\tau) = B_-(\tau) = \psi^{(0)} = F_0 f(\tau), \tag{D 8}$$

$$A_+(\tau) - A_-(\tau) = -i\pi F_0 f(\tau). \tag{D 9}$$

The matching formula (D 9) shows the jump h_x through the resonance layer. Assuming $U_a^2(x) - 1 = [(\partial_\chi U_a^2)(x_0)]\chi$, the following formula for h_x is derived from (D 2) and (D 7) at $\Delta \ll |\chi| \ll L$:

$$h_x(\chi,\tau) = -i\frac{k_y^2}{k_z^2}\left[\partial_\chi U_a^2(x_0)\right]^{-1}\left[\left(A_{\pm}(\tau) + \frac{1}{2}B(\tau)\right) + B(\tau)\ln|\chi|\right].$$

If maching is given by (D 9), we have at $\Delta \ll \chi_0 \ll L$, $\chi_0 > 0$

$$h_x(\chi_0,\tau) - h_x(-\chi_0,\tau) = \Delta h_x(\tau) = -\pi k_y^2 F_0\left[\partial_x U_a^2(x_0)\right]^{-1} f(\tau). \tag{D 10}$$

https://doi.org/10.1017/S002237781000022X Published online by Cambridge University Press

The jump $\Delta h_x(\tau)$ is associated with a jump of the energy density flux Q_L. According to (2.10) and (D 10),

$$Q_L = -|F_0 f(\tau)|^2 k_y^2 \left|\left(\partial\chi U_a^2\right)(x_0)\right|^{-1}/2. \tag{D 11}$$

Appendix E

In the case of the localized large-scale mode, when neglecting the resonance absorption, we get real eigen frequencies ω_n and their corresponding eigen modes $\Psi_{(0)}(\omega_n, \chi)$ of the zeroth approximation problem. Under action of the initial disturbance, each eigen mode of the zeroth approximation at $\tau = 0$ acquires a non-zero amplitude in the entire region of its localization, including the resonance layer. Assuming that the resonance absorption is small, let us express the large-scale disturbance in the form $\Psi = \mathbf{C}(\tau)\Psi_{(0)}(\omega_n, \chi) + \Psi_{(1)}(\omega_n, \chi, \tau)$, where $\Psi_{(1)}$ is the small addition responsible for taking the resonance absorption into account. As $\Psi_{(1)} \to 0$ as $Q_L \to 0$, we way assume that $|\Psi_{(1)}| \ll |C(\tau)\Psi_{(0)}|$ in the case of small resonance absorption. Then $\Psi \approx C(\tau)\Psi_{(0)}$ and $\Psi \approx C(0)\Psi_{(0)}$ when $\tau \to 0$. Therefore, within the frame of the zeroth approximation, in addition to the frequency, we can determine amplitude that the large-scale localized mode obtains under action of an arbitrary initial disturbance, choosing $C(0) = 1$, as equal to the zeroth-approximation mode amplitude. Hence, we determine $\psi^{(0)}$ at $\tau = 0$. Let us find time dependence $\psi^{(0)}$, assuming that energy density flux of the large-scale mode into the resonance layer is given by (D 11). Energy density of the large-scale mode integrated on the coordinate along the inhomogeneity can be represented as $\varepsilon = |\psi^{(0)}|^2 \varepsilon_0$, where ε_0 is independent of τ. The energy conservation law gives $\partial_\tau \varepsilon = -Q_F$. Hence, we get $f(\tau) \propto \exp[-\gamma\tau]$.

References

Abramovitz, M. J. and Stegan, I. 1970 *Handbook of Mathematical Functions.* New York, NY: Dover Publishing Co.

Akhiezer, A. I., Akhiezer, I. A., Polovin, R. V., Sitenko, A. G. and Stepanov K. N. 1974 *Plasma Electrodynamics.* Moscow: Nauka.

Chen, L. and Hasegawa, A. 1974 Plasma heating by spatial resonance of Alfven waves. *Phys. Fluids* **17**, 1399–1403.

Dmitrienko, I. S. 1999 Nonlinear non-stationary Alfven resonance. *J. Plasma Phys.* **62**, 145–164.

Einaudy, G. and Mok, J. 1985 Resistive Alfven normal modes in a nonuniform plasma. *J. Plasma Phys.* **34**, 259–270.

Goertz, G. K. and Boswell, R. W. 1979 Magnetosphere-ionosphere coupling. *J. Geophys. Res* **84**(A12), 7239–7246.

Goossens, M., Ruderman, M. S. and Hollweg, J. V. 1995 Dissipative MHD solutions for resonant Alfven waves in 1-dimensional magnetic flux tubes. *Sol. phys. J.* **157**, 75–102.

Hasegawa, A. and Chen, L. 1976 Kinetic processes in plasma heating by resonant mode conversion of Alfven. *Phys. Fluids* **19**, 1924–1976.

Ionson, J. A. 1978 Resonant absorption of Alfvenic surface waves and heating of solar coronal loops. *Astrophys. J.* **226**, 650–673.

Olver, F. W. J. 1974 *Asymptotics and Special Functions.* New York, NY: Academic Press.

Ruderman, M. S., Tirry, W. and Goossens, M. (1995) Non-stationary resonant Alfven surface waves in one-dimentional magnetic plasmas. *J. Plasma Phys.* **54**, 3129–3148.

https://doi.org/10.1017/S002237781000022X Published online by Cambridge University Press

Southwood, D. G. 1974 Some feature of field line resonances in the magnetosphere. *Planet. Space Sci.* **22**, 483–491.

Stasiewicz, K., Bellan, P., Chaston, C., Kleitzing, C., Lysak, R., Maggs, J., Pokhotelov, O., Seyler, C., Shukla, P., Stenflo, L., Streltsov, A. and WaHlund, J-E. 2000 Small-scale Alfvenic structure in the Aurora. *Space Sci. Rev.* **92**, 423–533.

Stefan, J. R. 1970 Alfven wave damping from finite gyroradius coupling to the ion acoustic mode. *Phys. Fluids.* **13**(A12), 440.

Swanson, D. J. 1975 Mode conversion of toroidal Alfven waves. *Phys. Fluids* **18**, 1269–1276.

Tirry, W. J. and Goossens, M. 1996 Quasi-modes as dissipative magnetohydrodynamic eigenmodes: Results for one-dimensional equilibrium states. *Astrophys. J.* **471**, 501–509.

https://doi.org/10.1017/S002237781000022X Published online by Cambridge University Press